Microfluidic pumps employing surface acoustic waves generated in ZnO thin films

X. Y. Du,[1] Y. Q. Fu,[1,2] J. K. Luo,[1,3,a)] A. J. Flewitt,[1] and W. I. Milne[1]

[1]*Electrical Engineering Division, Department of Engineering, University of Cambridge, JJ Thomson Ave., Cambridge CB3 0FA, United Kingdom*
[2]*Department of Mechanical Engineering, School of Engineering and Physical Sciences, Heriot-Watt University, Edinburgh EH14 4AS, United Kingdom*
[3]*Centre for Material Research and Innovation, University of Bolton, Deane Road, Bolton BL3 5AB, United Kingdom*

ZnO thin film based surface acoustic wave (SAW) devices have been utilized to fabricate microfluidic pumps. The SAW devices were fabricated on nanocrystalline ZnO piezoelectric thin films deposited on Si substrates using rf magnetron sputtering and use a Sezawa wave mode for effective droplet motion. The as-deposited ZnO surface is hydrophilic, with a water contact angle of $\sim 75°$, which prevents droplet pumping. Therefore, the ZnO surface was coated using a self-assembled monolayer of octadecyltrichlorosilane which forms a hydrophobic surface with a water contact angle of $\sim 110°$. Liquid droplets between 0.5 and 1 μl in volume were successfully pumped on the hydrophobic ZnO surface at velocities up to 1 cm s^{-1}. Under acoustic pressure, the water droplet on an hydrophilic surface becomes deformed, and the asymmetry in the contact angle at the trailing and leading edges allow the force acting upon the droplet to be calculated. These forces, which increase with input voltage above a threshold level, are found to be in the range of ~ 100 μN. A pulsed rf signal has also been used to demonstrate precision manipulation of the liquid droplets. Furthermore, a SAW device structure is demonstrated in which the ZnO piezoelectric only exists under the input and output transducers. This structure still permits pumping, while avoiding direct contact between the piezoelectric material and the fluid. This is of particular importance for biological laboratory-on-a-chip applications. © 2009 American Institute of Physics.
[DOI: 10.1063/1.3068326]

I. INTRODUCTION

Surface acoustic wave (SAW) devices have been in commercial use for more than 60 years, with their main applications in communications (filters and oscillators in mobile phone or televisions); automotive sensors (torque and tire pressure), environmental sensors (chemical, vapor, humidity), and other industrial and commercial sectors.[1–3] Recently, there has been an increased interest in SAW-based biosensors and microfluidic systems using high performance piezoelectric materials, such as LiNbO$_3$.[4–6] SAW-based biochemical sensors normally have high sensitivity and low detection limits in the order of a few pg/ml. In order to detect the existence of biological species such as cancer cells, proteins, or DNA, it is essential to handle and manipulate small quantities of fluids (both reagents and specimens) to immobilize and to bind the target molecules on the surface of the biosensor. Handling of such small volumes of liquid as a droplet forms a key challenge.

Various microfluidic pumps and mixers have been developed to control, manipulate, and mix the minute amount of liquid in microliter to picoliter volumes, including devices based on mechanical moving parts (such as oscillating membranes), electric fields applied to liquids, magnetic fields ap-

plied to fluids or inducing phase changes in fluids.[7,8] SAW-based pumps and mixers have distinct advantages, such as simple device structure with no moving parts, low fabrication cost, electronic control, high speed, programmable, no physical contact between the electrodes and the liquids to be manipulated, compactness, high frequency response, and the ability to arbitrarily manipulate fluids on a flat surface with precision.[9–12]

The surface acoustic wave is generated by applying a rf signal to a set of interdigitated transducers (IDTs) which lie on top of a piezoelectric material. The piezoelectric materials may be the bulk of the substrate, such as lithium niobate (LiNbO$_3$) or simply be a thin film material on the surface of a substrate, such as a zinc oxide (ZnO) film on a silicon substrate. When the frequency, f, of the rf signal is equal to v_S/p, where v_S is the acoustic velocity of the substrate/piezoelectric system and p is the periodic spacing of the IDT electrodes, then constructive interference occurs and an intense acoustic wave is generated which travels through the piezoelectric substrate. The mode of the acoustic wave is determined by the crystallographic orientation of the piezoelectric material and, in the case of devices using a thin film piezoelectric, the thickness of the piezoelectric layer.[13] For microfluidic applications, a component of the acoustic wave is required in the direction of propagation, and the so-called Rayleigh mode is commonly employed in which an individual atom performs elliptical motion in the plane perpen-

a)Author to whom correspondence shoul be addressed. Electronic mail: j.luo@bolton.ac.uk
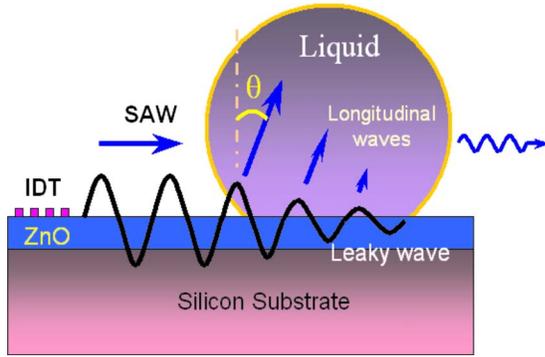
FIG. 1. (Color online) Schematic drawing of interaction between surface acoustic wave and a liquid droplet and defining the Rayleigh angle, θ.

dicular to the surface and parallel to the direction of propagation. However, the excessive damping of the Rayleigh mode by the liquid means that this mode is considered to be unsuitable for sensing applications.[14–16]

The coupling of the acoustic wave into liquid on the surface of the SAW device, which is required for pumping or mixing, occurs through the excited longitudinal waves propagating into the liquid at an angle called the Rayleigh angle, following the Snell law of diffraction (see Fig. 1).[17–19] The Rayleigh angle, θ, is defined by

$$\theta = \sin^{-1}\left(\frac{v_L}{v_S}\right), \qquad (1)$$

where v_L is the velocity of the longitudinal wave in the liquid. However, the energy and the momentum of the longitudinal wave radiated into the liquid are quite useful for liquid pumping and mixing. Indeed, liquid streaming, movement, and even ejection (atomization) have been demonstrated on LiNbO$_3$ SAW devices upon gradual increase of the wave amplitude.[20–23] A net pressure gradient, P, forms in the direction of the acoustic wave propagation and provides an effective force to drive the liquid, which can be described by[24]

$$P = \rho_o v_s^2 \left(\frac{\Delta\rho}{\rho_o}\right)^2, \qquad (2)$$

in which, ρ_o is the liquid density and $\Delta\rho$ is the slight density change due to the acoustic pressure. Based on the acoustic streaming effect, microfluidic pump and mixer systems,[25–28] droplet positioning and manipulation systems,[29,30] atomization systems,[31] fluidic dispenser arrays,[30] and acoustic ejectors[32] have all been proposed and developed.

Most of the SAW devices so far have been made from bulk piezoelectric materials, such as LiNbO$_3$ and quartz. Bulk piezoelectric materials are expensive, and cannot be integrated with control electronics, preventing them from widespread application in microfluidics. On the other hand, thin film ZnO has good piezoelectric properties, a high electromechanical coupling coefficient, high sensitivity, and reliability.[33] Furthermore, it can be deposited by such methods as rf magnetron sputtering and laser-assisted deposition on a variety of substrates, including silicon, making it the most promising material for integration with electronic control circuitry.[34,35] Such integration is the prerequisite for a

fully automated and digitized microsystem with low cost, fast speed, reduced reagent requirement, and precision control of liquid quantity and position. However, little effort has been made to develop SAW microfluidic systems using piezoelectric thin films such as ZnO or AlN. The authors have recently successfully demonstrated acoustic mixing using the SAW devices made on ZnO thin films, and have obtained a within-droplet streaming velocity of up to 5 cm s^{-1} using a Sezawa wave (high order Rayleigh mode) in the devices.[12,36] This paper reports on the effect of a self-assembled monolayer of octodecyltrichlorosilane (OTS) coating on hydrophobicity properties of ZnO film surfaces. Consequently, microfluidic pumping is achieved rather than mixing alone. Observation of microcontact angle allows the force acting on water droplets to be determined and general principles for the requirements of hydrophobic surfaces for microfluidic pumps to be established. A SAW structure design is also proposed and demonstrated in which the piezoelectric ZnO thin film is only under the IDTs and not in the pumping region, which is particularly attractive for laboratory-on-a-chip applications.

II. EXPERIMENTAL PROCEDURE

The fabrication of the IDT structures has been previously described in detail by the authors in Refs. 12 and 42. Thin films of ZnO up to 6.6 μm thick were deposited onto Si(100) substrates by rf magnetron sputtering. The IDT transducers were then fabricated from rf magnetron sputtered aluminum thin films up to 150 nm thick. This was sufficiently thin to avoid significant mass loading effects.[37] The resulting IDTs consisted of 30 or 60 pairs of fingers, with a period, p, of 32 μm, and an aperture (active IDT width) of 4900 μm. An HP8711A rf network analyzer was used to characterize the SAW devices. The propagation of the SAW was studied through the analysis of the scattering parameters in two configurations: S_{11} and S_{22} (reflection) and S_{21} and S_{12} (transmission). The rf signal from an Agilent N9310A signal generator was amplified by a power amplifier up to a peak-to-peak value of 70 V before being fed into the IDTs. The amplitudes of the signals or input voltages were checked using an oscilloscope (Tektronix TDS). Water droplets with different sizes were obtained using a Micro-Volume Kit micropipette. Droplet movement was measured using a video camera (Motic MCCamera) using both top and horizontal views.

III. RESULTS AND DISCUSSIONS

A. Measurement of acoustic force

ZnO is hydrophilic with a contact angle typically at 30°–75°, which is strongly dependent on the surface conditions and light exposure.[38] The contact angle increases with the ZnO film thickness as the roughness of the ZnO films increases with the thickness. The typical contact angle for a clean surface is between 70° and 80°. The hydrophilic nature of the surface has the effect of preventing pumping of water droplets on the SAW device. Instead, streaming only is observed within the droplet, which the authors have reported previously.[36] Additionally, the droplet deforms so that the contact angle on the "trailing edge" of the drop, θ_t (closest to
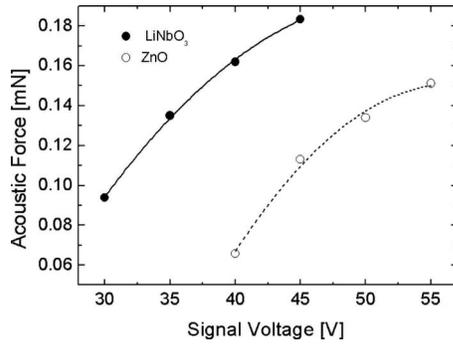
FIG. 2. Acoustic force as a function of rf signal voltage acting on a 10 μl water droplet for both a LiNbO$_3$ (Ref. 42) and ZnO SAW device. The LiNbO$_3$ device uses a Rayleigh mode wave, while the ZnO device uses a Sezawa mode wave. Both devices have 60 finger pairs in the IDT.

the driving IDT) is reduced, while that on the leading edge, θ_l, is increased. The acoustic force, F_s, can be calculated from the asymmetry in these contact angles and the droplet size from,[39–41]

$$F_s = 2R\gamma_{LG}\sin\left(\frac{\theta_t + \theta_l}{2}\right)(\cos\theta_t - \cos\theta_l), \qquad (3)$$

where R is the radius of the droplet and γ_{LG} is the liquid-gas surface energy.

Figure 2 shows the dependence of acoustic force generated on a 10 μl water drop by the Sezawa wave from the ZnO piezoelectric as a function of rf signal voltage (peak to peak), as well as the acoustic force produced by a Rayleigh wave from a LiNbO$_3$ SAW IDT that the authors have reported.[42] It was found that, under conditions where a Rayleigh mode wave was induced in the ZnO, the acoustic force generated was insufficient to deform the droplet, whereas when the Sezawa mode wave was generated, significant droplet deformation was observed, indicating a far high acoustic force. This contrasts with the observations for LiNbO$_3$ SAW devices[42] where the fundamental Rayleigh mode wave only has sufficient force to deform the droplet. The key difference between the two devices is that, while the ZnO piezoelectric is a thin film material on a silicon substrate, the LiNbO$_3$ is a bulk piezoelectric wafer. This indicates that different wave modes are required for microfluidic pumps fabricated from bulk and thin film piezoelectrics where, in the latter case, the acoustic wave has a certain proportion confined to the thin film region.

Figure 2 also shows that a threshold voltage, V_{th}, is required before droplet deformation is observed. Thereafter, it is found that the force increases with the input voltage, but has a tendency to saturate at high values of voltage. The rolling-off in acoustic force with increasing power is attributed to temperature-induced frequency shifts at high power.[42–44] It is known that the transmitted acoustic wave amplitude, T, has the form

$$T = \gamma\left(\frac{\sin(\Delta f)}{\Delta f}\right)^2, \qquad (4)$$

where Δf is the deviation in frequency from the resonant frequency and γ is a constant. It may reasonably be assumed that the power fed into the acoustic wave is proportional to

TABLE I. Extracted parameters for the acoustic force extraction.

Material	α (mN V^{-2})	β (V^{-1})	V_{th} (V)
LiNbO$_3$	$(3.28 \pm 0.08) \times 10^{-5}$	0.042 ± 0.006	11 ± 3
ZnO	$(5 \pm 2) \times 10^{-4}$	0.055 ± 0.011	27 ± 3

$(V-V_{th})^2$, and that this has two effects. First, it will increase the amplitude of the acoustic wave, and hence the force acting on the droplet. Second, it will cause the system to heat up, resulting in a shift in the resonant frequency. Assuming that this shift is also proportional to the input power, then these effects may be combined in a single expression for the acoustic force as a function of input voltage,

$$F_s = \alpha(V - V_{th})^2\left(\frac{\sin[\beta(V - V_{th})]}{\beta(V - V_{th})}\right)^2, \qquad (5)$$

where α is a force-voltage coupling coefficient and β is the constant of proportionality relating the input voltage to the temperature-induced frequency shift. Figure 2 shows the fitted curve for each case, and Table I shows the fitting parameters. It is noticeable that the force-voltage coupling coefficient is greater for ZnO as well as the temperature-induced frequency shift coefficient. The threshold voltage is also much greater in the ZnO device, and is most likely a result of the ZnO being a polycrystalline thin film compared to the bulk single crystal LiNbO$_3$. The former has a limited piezoelectric effect. The upper limit of the signal voltage for the LiNbO$_3$ SAW device is 45 V, above which the LiNbO$_3$ device cracks along the IDTs and fails to operate because of localized heating effect at the electrodes. No such cracking was observed in the ZnO SAW devices up to 70 V, probably due to the higher thermal conductivity of the Si substrate. At extremely high signal voltages (>60 V), a stream of tiny droplets with sizes in the range from a few fl to pl are generated and ejected from the ZnO SAW device.

B. Microfluidic pumping on hydrophobic surfaces

For droplet manipulation on a channelless flat surface, the surface of the SAW devices was modified to obtain a hydrophobic surface. A self-assembled monolayer (SAM) of octadecyltrichlorosilane (OTS) monolayer was found to be one of the best materials for this purpose. The process to form an OTS SAM layer involved immersing the sample in a toluene solution of OTS (0.01 mM) for 6 h at room temperature and then baking it for 1 h at 125 °C. The IDT electrodes were covered by photoresist (AZ5214E) to avoid Al electrode corrosion by the OTS solution. Once the SAM formation was completed, the photoresist was removed by immersing the sample in acetone in which the OTS SAM layer is stable. The OTS SAM layer exhibits excellent uniformity and good adhesion to the substrate. The average thickness of the OTS film is $\sim$10 nm which induces no measurable acoustic damping.

After the ZnO surface was modified by the OTS, the contact angle of the water droplet increased from $\sim$75° to $\sim$110°, as shown in Fig. 3, largely depending on the process
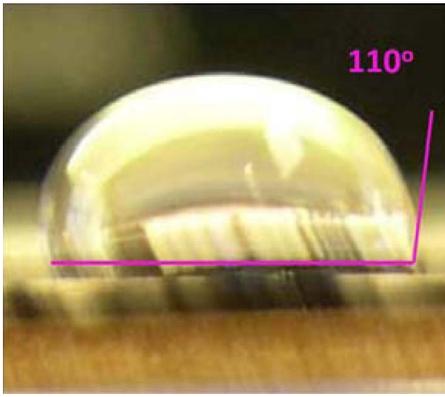
FIG. 3. (Color online) Photos of a droplet on an untreated and an OTS treated ZnO surface. The contact angle increased from ~75° to 110° after OTS SAM layer formation.

conditions. The OTS treated surface of the ZnO SAW is very stable and remains hydrophobic with the same contact angle even after several weeks.

Increasing the contact angle of a liquid droplet on a solid surface by making the surface hydrophobic also reduces the work of adhesion, W_s, of the droplet on the surface.[45] For any liquid on a surface, the work of adhesion is related to the contact angle, θ, and the liquid-gas surface free energy, γ_{LG}, by

$$W_S = \gamma_{LG}(1 + \cos\,\theta), \tag{6}$$

where γ_{LG} is 72.9 mN m^{-1} for water at room temperature in air. This is the force per unit length acting at the line of contact between the air, liquid, and solid. Therefore, the total acoustic force that must be applied to the droplet to cause pumping must be greater than the force acting along the length ($2\pi R \sin\,\theta$) of this line of contact, F_c, which can be calculated to be

$$F_c = \gamma_{LG}(1 + \cos\,\theta)2\pi R \sin\,\theta, \tag{7}$$

where the radius of the droplet, R, may be simply calculated from its volume, V, by

$$V = \frac{\pi R^3}{3}(2 + \cos\,\theta)(1 - \cos\,\theta)^2. \tag{8}$$

Figure 4 shows how F_c varies as a function of contact angle for a 10 μl droplet of water on a surface. It is clear that
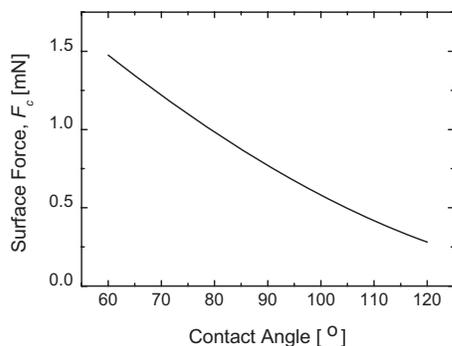
FIG. 4. Variation in minimum acoustic force, F_c, required to move a water droplet of 10 μl volume on a surface as a function of contact angle calculated from Eqs. (6) and (7).
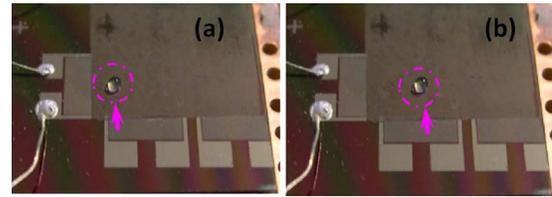
FIG. 5. (Color online) Photos of a 1 μl droplet movement on an OTS treated ZnO SAW device before (a) and after (b) being driven by a rf signal at a frequency of 178.7 MHz.

reducing the contact angle from ~75° to 110° results in a reduction in the work of adhesion by almost an order of magnitude, from well in excess of 1.5 mN to ~400 μN. This is the force that would be required to detach the droplet from the surface completely. The force required to simply move the droplet will be some fraction of the work of adhesion. It has already been shown in Sec. III A that the acoustic force that can be generated using the SAW devices in this study is ~100 μN for a 10 μl droplet. The exact mechanism of droplet motion is not clear yet, but two possible mechanisms are suggested here. First, under such a strong acoustic force the droplet deforms with an increased leading edge contact angle and decreased trailing edge contact angle, as shown in a previous publication by the authors.[42] The increased surface energy of the droplet on the hydrophobic surface makes the contact angle of the trailing edge return to its original value, which reduces the contact area, while the conservation of the work of adhesion of the droplet makes the leading angle decrease by expanding the droplet area a little in front, hence moving the droplet forward a little. By applying a "continuous" rf wave, a constant droplet velocity appears to result. This pumping process is similar to that of electrowetting,[46,47] but in a reversed order (i.e., the droplet moves in the increased contact angle direction under the acoustic force). The second possible mechanism is that, under the application of the rf wave, the deformed droplet vibrates, and may expand a little in forward direction owing to the acoustic force, hence moving the droplet forward.

Figure 5 shows photos of a 1 μl droplet before and after applying a rf signal at 178.7 MHz to the ZnO SAW device with a peak-to-peak voltage of 40 V for a duration of 2 s. The water droplet is observed to have moved a distance of ~4 mm. Figure 6 shows the dependence of droplet velocity as a function of rf signal voltage. Unsurprisingly, this graph
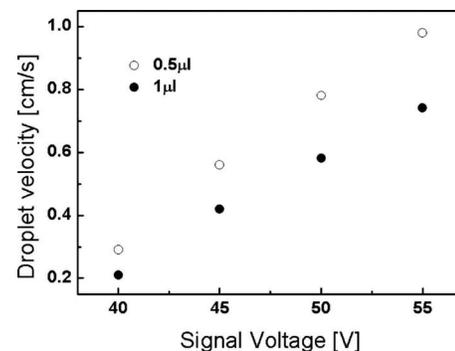
FIG. 6. Sezawa wave driven droplet velocity as a function of rf signal voltage applied on the SAW for a 5.5 μm ZnO SAW device.
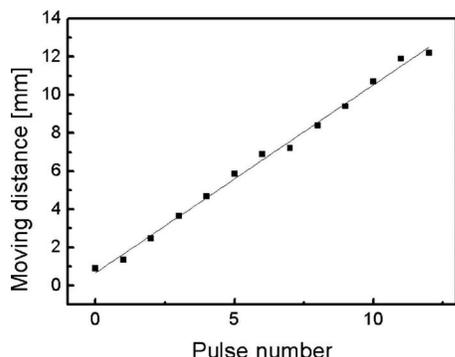
FIG. 7. Total distance moved by a 0.5 μl water droplet as a function of pulse number for a rf signal of 40 V and a pulse width of 100 ms.

FIG. 8. (Color online) Schematic drawing of the proposed SAW structure with ZnO on the wave path being removed compared with the standard SAW device structure where the ZnO is not patterned.

shows a similar form to that found for acoustic force as a function of input voltage (Fig. 2). Smaller droplets are found to have a higher velocity for the same input voltage due to their reduced work of adhesion. The droplet velocities achieved on ZnO are about half those reported previously by the authors on LiNbO$_3$,[42] but are larger than those of most micropumps and are sufficient for microfluidic applications.

Practically, a pulsed rf signal is normally used to control the droplet motion, as this affords more precise control of the position and moving distance while also suppressing acoustic heating. Figure 7 shows the dependence of the moving distance of a 0.5 μl water droplet as a function of pulse number applied. The rf signal voltage is 40 V and the pulse width is 100 ms. The total distance moved increases linearly with the number of pulses applied. The average distance moved per pulse is nearly 100 μm, although this is strongly dependent on the signal voltage and the droplet size.

C. Island structure SAW devices

Although ZnO is not biologically toxic, it is very reactive with acids or bases[48] and will dissolve or recrystallize if exposed to water or a humid environment.[49] Therefore, ZnO SAW devices with no surface protection are not suitable for laboratory-on-a-chip applications. Surface coating is considered to be one way of protecting ZnO thin films from degradation. However, in this work a ZnO SAW structure is proposed which can avoid a direct contact between the ZnO active layer and the fluid being pumped altogether.

Since the acoustic wave in a thin film ZnO SAW device is strongly affected by wave propagation in the Si substrate, it is proposed that the two functions of SAW generation and propagation can be separated. The proposed device structure is shown in Fig. 8. The ZnO is patterned into islands so that it only exists underneath the IDTs where piezoelectric material is required for SAW generation or sensing. The base silicon substrate is then used for SAW propagation.

Figure 9 is a comparison of both Rayleigh and Sezawa mode transmission spectra of SAW devices with and without a ZnO propagation path. The SAW devices were made on the ZnO film coated Si substrates first, and then the ZnO film between the two opposite IDTs was etched by Al etchant to expose the Si substrate. It was found that the transmission spectrum depends on the thickness of the piezoelectric active layer. For the SAW device on a 1.2 μm ZnO film, the abso-

lute value of the transmitted signal of the Rayleigh and Sezawa mode waves decreases after removing the ZnO in the propagation region. However, a signal is still clearly observed in both cases that is well above the level of system noise.
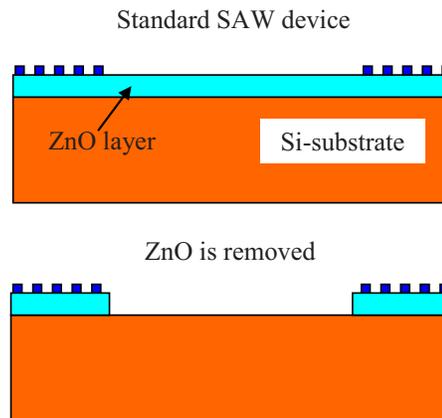
The resonant SAW frequency is determined by the IDT periodicity and the acoustic speeds in the substrate and thin film overlayer in the region of the IDTs—it is not strongly affected by the active layer in the propagation region. For a layered structure, the longitudinal acoustic waves travel with a certain proportion of the waves existing in each of the thin film surface layer and the bulk substrate. Since the wavelength in this case is ~ 32 μm, which is much greater than the thickness of the 1.2 μm ZnO thin film, it might be expected that the acoustic energy mainly exists within the silicon substrate, and that the removal of such a thin layer in the propagation region would not affect the transmission signal significantly. However, the lower acoustic velocity of the ZnO (~ 2700 m s^{-1}) relative to the silicon substrate (~ 4680 m s^{-1}) means that there will be a tendency for enhanced wave trapping.[42,50] This is particularly true for the Sezawa wave mode, which is known to be more confined to the surface. Further increase in the ZnO thickness means a higher proportion of acoustic waves, and hence energy, is trapped within the active layer. This explains the significant decrease in transmission signal observed upon removal of the ZnO layer—an effect that is particularly pronounced for the Sezawa mode wave.

This reduction in transmitted signal also results in a reduced acoustic force that can act upon microfluidic droplets. Figure 10 shows the streaming velocity that occurs within a droplet of water that is exposed to the acoustic wave, but where the surface is hydrophilic so that no pumping motion occurs (the methodology for conducting this experiment has been previously described by the authors in Ref. 42). Streaming velocities are obtained that are $\sim 60\%$ lower compared to devices with a continuous ZnO layer, but are still significant, and indicates that these devices can still be effectively used for microfluidic applications.
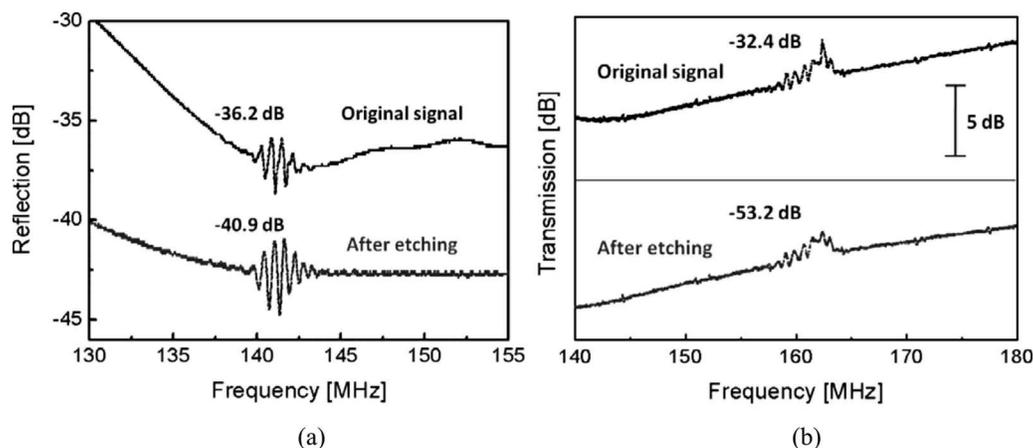
FIG. 9. Comparison of transmission spectra for SAW devices before and after removal of the ZnO from the propagation area using (a) the Rayleigh wave from a 1.2 μm thick ZnO thin film and (b) the Sezawa wave from a 6.6 μm thick ZnO thin film.

D. Acoustic heating

Acoustic heating is a common phenomenon in SAW-based devices, and will affect the performance of acoustic streaming and pumping significantly.[51,52] First, increasing temperature shifts the resonant frequency of a SAW device, which is normally taken as a constant in SAW microfluidics. Second, it introduces errors in sensing using the SAW devices, as changes in transmission amplitude and resonant frequency are no longer solely a function of mass loading. Third, the heat may damage the integrity of biological substances to be tested. In order to quantify this effect, the surface temperature of the SAW devices have been investigated by using a thermocouple to measure the temperature change on the ZnO film surface. Measurements were performed without any liquid on the SAW device surface.

Figure 11 shows the temperature change in the ZnO film surface (5 mm away from the IDT) measured as a function of duration and peak-to-peak voltage of the input rf signal. It is apparent that the surface temperature of the ZnO SAWs increases with increase in the voltage and duration of the rf signal. The maximum temperature recorded was ~140 °C for the highest signal voltage of 60 V. Hence, the previous observation of bubble formation and evaporation of the wa-

ter droplets during ZnO SAW microfluidic studies can be attributed to the acoustic heating effect, although the presence of liquid on the SAW surface will undoubtedly result in a lower temperature during microfluidic operation than those measured here.

The acoustic heating can be significantly reduced by using a pulsed rf signal. The surface temperature of the device was found to remain constant at room temperature with a pulse width up to 200 ms and peak-to-peak magnitude of 45 V owing to heat dissipation during the off period of the pulsed rf signal, and a slight increase in temperature up to ~40 °C was observed when the pulse width increased to 600 ms. A pulsed rf signal also has the advantage of inducing effective mixing because of the nonregular streaming patterns, and precise control of droplet motion as discussed in Sec. III B.

IV. CONCLUSIONS

ZnO thin film based SAW micropumps have been fabricated based on low cost, high quality, *c*-axis oriented ZnO thin films deposited on silicon substrates using a rf magnetron sputtering system. The results showed that droplet manipulation on the ZnO device depends on the SAW ampli-
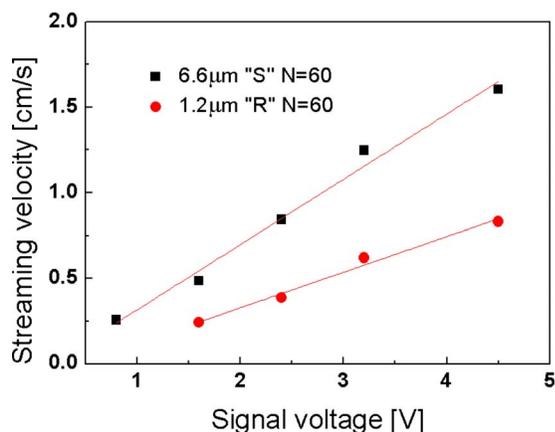
FIG. 10. (Color online) Streaming velocity induced by acoustic waves from the SAW devices where there is no ZnO in the propagation region. Results for both Sezawa (s) and Rayleigh (r) mode devices are presented.
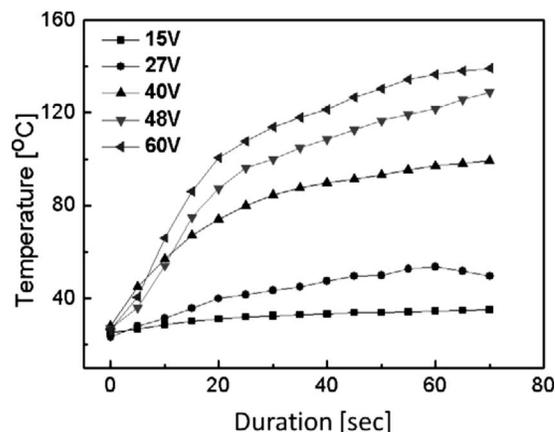
FIG. 11. Temperature change as a funciton of time with rf signal voltage as a parameter. The temperature rises rapidly at the initial 20 s, and then increases slowly thereafter.

tude, wave mode, droplet size, and surface hydrophobicity of the substrate. Acoustic forces ~100 μN were produced, and it has been shown that this is sufficient to induce pumping of 10 μl water droplets where the surface contact angle is significantly greater than 100°. This can be achieved by using OTS to modify the ZnO surface to form a hydrophobic coating with a water contact angle of ~110°. Pumping velocities approaching 1 cm s^{-1} were measured. A pulsed rf signal has also been used to demonstrate precision manipulation of the liquid droplets. Furthermore a SAW device on ZnO island structure has been proposed, fabricated and microfluidic operation verified. This structure avoids a direct contact between the piezoelectric material and microfluidic substances, and hence is promising for laboratory-on-a-chip applications.

ACKNOWLEDGMENTS

[1] D. S. Ballantine, R. M. White, S. J. Martin, A. J. Ricco, E. T. Zellers, G. C. Frye, and H. Wohltjen, *Acoustic Wave Sensor: Theory, Design, & Physico-Chemical Applications* (Academic, New York, 1996).

[2] M. Hoummady, A. Campitelli, and W. Wlodarski, Smart Mater. Struct. **6**, 647 (1997).

[3] D. W. Galipeau, P. R. Sory, K. A. Vetelino, and R. D. Mileham, Smart Mater. Struct. **6**, 658 (1997).

[4] M. J. Vellekoop, Ultrasonics **36**, 7 (1998).

[5] S. Shiokawa and J. Kondoh, Jpn. J. Appl. Phys., Part 1 **43**, 2799 (2004).

[6] E. Gizeli, Smart Mater. Struct. **6**, 700 (1997).

[7] N.-T. Nguyen, X. Huang, and T. K. Chuan, J. Fluids Eng. **124**, 384 (2002).

[8] C. S. Zhang, D. Xing, and Y. Y. Li, Biotechnol. Adv. **25**, 483 (2007).

[9] Z. Guttenberg, H. Muller, H. Habermuller, A. Geisbauer, J. Pipper, J. Felbel, M. Kielpinski, J. Scriba, and A. Wixforth, Lab Chip **5**, 308 (2005).

[10] A. Renaudin, P. Tabourier, J.-C. Camart, and C. Druon, J. Appl. Phys. **100**, 116101 (2006).

[11] A. Renaudin, P. Tabourier, V. Zhang, J.-C. Camart, and C. Druon, Sens. Actuators B **113**, 389 (2006).

[12] X. Y. Du, Y. Q. Fu, S. C. Tan, J. K. Luo, A. J. Flewitt, S. Maeng, S. H. Kim, Y. J. Choi, D. S. Lee, N. M. Park, J. Park, and W. I. Milne, J. Phys.: Conf. Ser. **76**, 012035 (2007).

[13] J. W. Gardner, V. K. Varadan, and O. O. Awadelkarim, *Microsensors, MEMS and Smart Device* (Wiley, New York, 2001).

[14] H. L. Bertoni and T. Tamir, Appl. Phys. **2**, 157 (1973).

[15] S. Shiokawa, Y. Matsui, and T. Ueda, J. Appl. Phys. **29**, 137 (1990).

[16] M. I. Newton, M. K. Banerjee, T. K. H. Starke, S. M. Bowan, and G. McHale, Sens. Actuators, A **76**, 89 (1999).

[17] A. Wixforth, Superlattices Microstruct. **33**, 389 (2003).

[18] S. Shiokawa, Y. Matsui, and T. Morizum, Jpn. J. Appl. Phys., Part 1 **28**, 126 (1989).

[19] T. Koga and M. Morita, Langmuir **21**, 905 (2005).

[20] S. Shiokawa, Y. Matsi, and T. Morizumi, Jpn. J. Appl. Phys., Part 1 **28**, 126 (1989).

[21] J. C. Rife, M. I. Bell, J. S. Horwitz, M. N. Kabler, R. C. Y. Auyeung, and W. J. Kim, Sens. Actuators, A **86**, 135 (2000).

[22] A. Wixforth, J. Assoc. Lab. Autom. **11**, 399 (2006).

[23] S. Alzuaga, S. Ballandras, F. Bastien, W. Daniau, B. Gauthier-Manuel, J. F. Manceau, B. Cretin, P. Vairac, V. Laude, A. Khelif, and R. Duhamel, Proc.-IEEE Ultrason. Symp. **2**, 1790 (2003).

[24] M. Rotter, A. V. Kalameitsev, A. O. Govorov, W. Ruile, and A. Wixforth, Phys. Rev. Lett. **82**, 2171 (1999).

[25] W. K. Tseng, J. L. Lin, W. C. Sung, S. H. Chen, and G. B. Lee, J. Micromech. Microeng. **16**, 539 (2006).

[26] A. Toegl, R. Kirchner, C. Gauer, and A. Wixforth, J. Biomol. Tech. **14**, 197 (2003).

[27] K. Sritharan, C. J. Strobl, M. F. Schneider, and A. Wixforth, Appl. Phys. Lett. **88**, 054102 (2006).

[28] W. K. Tseng and J. L. Lin, J. Micromech. Microeng. **16**, 539 (2006).

[29] A. Sano, Y. Matsui, and S. Shiokawa, Jpn. J. Appl. Phys., Part 1 **37**, 2979 (1998).

[30] C. J. Strobl, Z. V. Guttenberg, and A. Wixforth, IEEE Trans. Ultrason. Ferroelectr. Freq. Control **51**, 1432 (2004).

[31] K. Chono, N. Shimizu, Y. Matsu, J. Kondoh, and S. Shiokawa, Jpn. J. Appl. Phys., Part 1 **43**, 2987 (2004).

[32] J. W. Kwon, H. Yu, Q. Zou, and E. S. Kim, J. Micromech. Microeng. **16**, 2697 (2006).

[33] S. J. Pearton, D. P. Norton, K. Ip, Y. W. Heo, and T. Steiner, Prog. Mater. Sci. **50**, 293 (2005).

[34] W. Water and S. Y. Chu, Mater. Lett. **55**, 67 (2002).

[35] H. W. Kim and N. H. Kim, Phys. Status Solidi A **201**, 235 (2004).

[36] X. Y. Du, Y. Q. Fu, S. C. Tan, J. K. Luo, A. J. Flewitt, W. I. Milne, D. S. Lee, S. Maeng, S. H. Kim, N. M. Park, Y. J. Choi, J. Park, and Y. J. Choi, Appl. Phys. Lett. **93**, 094105 (2008).

[37] V. Laude, L. Robert, W. Daniau, A. Khelif, and S. Ballandras, Appl. Phys. Lett. **89**, 083515 (2006).

[38] G. Kenanakis, E. Stratakis, K. Vlachou, D. Vernardou, E. Koudoumas, and N. Natsarakis, Appl. Surf. Sci. **254**, 5695 (2008).

[39] D. Beyssen, L. Le Brizoual, O. Emazria, and P. Alnot, Proc.-IEEE Ultrason. Symp. **2**, 1028 (2005).

[40] C. G. L. Furmidge, J. Colloid Sci. **17**, 309 (1962).

[41] G. D. Yarnold, Proc. Phys. Soc. (London) **50**, 540 (1938).

[42] X. Y. Du, M. Swanwick, Y. Q. Fu, J. K. Luo, A. J. Flewitt, D. S. Lee, S. Maeng, and W. I. Milne, J. Micromech. Microeng. (unpublished).

[43] X. Q. Bao, W. Burkhard, V. Varadan, and V. K. Varadan, Proc.-IEEE Ultrason. Symp. **14–16**, 583 (1987).

[44] K. Tsubouchi and N. Mikoshiba, IEEE Trans. Sonics Ultrason. **32**, 634 (1985).

[45] A. Kawai and K. Suzuki, Jpn. J. Appl. Phys., Part 1 **45**, 5429 (2006).

[46] M. G. Pollack, R. B. Fair, and A. D. Shenderov, Appl. Phys. Lett. **77**, 1725 (2000).

[47] M. G. Pollack, A. D. Shenderov, and R. B. Fair, Lab Chip **2**, 96 (2002).

[48] B. A. Buchine, W. L. Hughes, F. L. Degertekin, and Z. L. Wang, Nano Lett. **6**, 1155 (2006).

[49] Y. Shu and D.F. Xue, Fourth International Conference on technol. advance of thin film & surf. coatings; Singapore, July 2008 (unpublished), pp. 92.

[50] E. Gizeli, Anal. Chem. **72**, 5967 (2000).

[51] J. Kondoh, N. Shimizu, Y. Matsui, and S. Shiokawa, IEEE Trans. Ultrason. Ferroelectr. Freq. Control **52**, 1881 (2005).

[52] R. G. Kryshtal, A. P. Kundin, A. V. Medved, and V. V. Shemet, Tech. Phys. Lett. **28**, 50 (2002).